JOURNAL OF AIRCRAFT
Vol. 45, No. 2, March–April 2008

Metrics for the Evaluation of Pedal Force/Feel Systems in Transport Aircraft

Ronald A. Hess*
University of California, Davis, Davis, California 95616-5294

DOI: 10.2514/1.32710

A piloted, fixed-base, simulation study was conducted at NASA Langley Research Center to determine optimum rudder pedal force/feel characteristics for transport aircraft. After completion of this simulation study, an evaluation of four metrics for assessing rudder pedal force/feel system characteristics previously presented in the literature was conducted. This evaluation was based upon the numerical handling-qualities ratings assigned to a variety of pedal force/feel systems used in the simulation study. It is shown that the majority of rudder pedal force/feel system configurations that received poor normalized pilot ratings also failed one or more of the metrics. In addition, the majority of configurations that received satisfactory normalized pilot ratings also passed all of the metrics. Based upon the simulation results, a fifth metric was identified that improved the ability of the complete set of metrics to identify poor force/feel system designs. It is suggested that these metrics could form the basis of a certification requirement for transport aircraft. One of the pilot-induced oscillations that occurred in the simulation was analyzed and a possible triggering event was identified.

I. Introduction

THE crash of American Airlines Flight 587 in November of 2001 led to a recommendation by the National Transportation Safety Board (NTSB) in October of 2004 to "...modify 14 CFR Part 25 to include a certification standard that will ensure safe handling qualities in the yaw axis throughout the flight envelope, including limits for rudder pedal sensitivity" [1]. This recommendation was issued to the Federal Aviation Administration (FAA). Unfortunately, no adequate database currently exists for determining such a certification standard. To begin establishing such a database, a piloted simulation study was conducted using the integrated flight deck (IFD) simulator at NASA Langley Research Center. The IFD facility is fixed-base in nature; that is, no motion cues are provided. However, the Langley IFD simulator cockpit included a stereo audio cue, the intensity of which was proportional to lateral acceleration at the pilot's station. The tone was directional (stereo) in nature and thus provided an aural cue related to the magnitude and direction of the lateral acceleration in the cockpit. The speakers that provided this cue can be seen on the left seat in Fig. 1, a view of the IFD cockpit taken from [2]. In addition, the IFD simulator has a wide field of view of approximately 200 deg, again visible in Fig. 1. Thus, large abrupt lateral disturbances resulted in significant visual cue changes, particularly in the periphery of the pilot's visual field.

The relative merits of static vs moving-base flight simulators have been discussed for some time (e.g., [3]), and the debate will not be reentered here. Indeed, other studies focusing upon rudder feel system characteristics have used moving-base simulation facilities (e.g., [4]). However, proprietary restrictions prevented the publication of quantitative results in [4]. The choice of a fixed-base cab was motivated here simply by the availability of the facility. That is, the Langley moving-base simulator was undergoing renovation during the period in which this study was conducted. Viewed in this light, the results of this study may be considered as a first step in developing design criteria for rudder force/feel systems and as an initial validation of the metrics to be described. The question of the extent to which lack of motion might have affected the ratings is a valid one. The tacit assumption here is that the relative ratings would remain reasonably unaffected by the absence of vestibular cues.

The characteristics of the rudder control system were examined in systematic detail. A preliminary discussion of the simulation results was presented in [2] and a complete report is in preparation. The aircraft simulated was a twin-engine, medium-sized transport. The task was a landing approach in crosswind and random turbulence. Severe lateral wind shear was introduced at heights ranging from 100 to 150 ft above ground level. No go-around or landing was allowed. The pilots were requested to track the runway centerline at 50 ft above ground level. A yaw damper was in operation in the simulation.

The choice of a landing approach task was motivated by a variety of factors. The task is obviously stressful, due to the proximity to the ground and the severe crosswinds that were encountered in the simulation. The presence of excellent visual cues provided by the runway was another factor; for example, aircraft heading changes and yaw rates were easily detected in the cockpit. However, the dynamic pressure associated with the flight condition was low (especially when compared with that encountered by American Airlines Flight 587 before loss of the vertical stabilizer). Thus, the task represented a compromise. It should be noted that investigation of a task with higher dynamic pressure would have made the lack of motion cues more crucial to the results.

Six different lateral wind-shear scenarios were presented, varying in magnitude and direction. Twelve active airline pilots participated in the study: seven males and five females. A total of 216 simulation runs were completed, not including those devoted to training and familiarization. Before discussing the pertinent subset of the results of the piloted simulation study, a review of four metrics for assessing the safety of rudder pedal force/feel systems in transport aircraft will be undertaken. It should be emphasized at the outset that the focus of this research summarized herein is different than that discussed in [2,4], in which *optimum* force/feel characteristics were sought. The goal here is the evaluation and possible refinement of metrics for identifying systems that may be unsafe. As used here, the adjective *unsafe* refers to systems that have the potential of initiating adverse pilot/vehicle interaction (e.g., the interaction leading to the structural failure that preceded the crash of American Airlines Flight 587).

II. Metric Definitions

Reference [5] suggested four metrics for assessing the safety of rudder pedal force/feel systems in transport aircraft:

Received 9 June 2007; revision received 28 September 2007; accepted for publication 28 September 2007.

*Professor, Department of Mechanical and Aeronautical Engineering. Associate Fellow AIAA.

Fig. 1 NASA Langley Research Center's IFD simulator cockpit from [2].

Metric 1 is a maximum value of required pedal force.

Metric 2 is a minimum value of a linearity index (LI) when applied pedal force is plotted vs pedal deflection in quasi-static fashion. Pedal forces and deflections from trim to maximum values are employed.

Metric 3 is minimum value of the linearity index when applied pedal force is plotted vs rudder deflection. The pedal force is a sinusoid yielding maximum pedal deflection at a frequency equal to the maximum Dutch-roll mode natural frequency in evidence across the flight envelope.

Metric 4 is a maximum value of lateral acceleration at the cockpit per pound of pedal force beyond breakout evaluated at a flight condition of maximum dynamic pressure.

Figure 2 and Eq. (1) define the simplified linearity index to be used in evaluating metrics 1 and 2. Initial estimates for each of the metric values are 1) the maximum required pedal force is 100 lbf, 2) LI > 0.7, 3) LI > 0.6, and 4) cockpit lateral acceleration less than 0.005 g/lbf.

$$\mathrm{LI} = 1 - \frac{\mathrm{area(HABH)} + \mathrm{area(GBCG)}}{\mathrm{area(HEBFH)}} \tag{1}$$

where H, A, B, etc., refer to points on the force/displacement diagram in Fig. 2.

In order, each of the metrics addresses a specific design issue in rudder pedal force/feel systems, including rudder actuators. Metric 1 suggests maximum required pedal forces based upon anthropometric data for males and females discussed in [5]. That is, the muscular strength of female subjects has been found to be about 67% that of males. The issue of maximum required pedal forces should reflect this difference in strength because female pilots are now common in transport aircraft cockpits. Metric 2 is based upon a pilot/vehicle analysis in [6] that suggested that highly nonlinear force/feel characteristics may lead to poor response predictability and tracking performance. The effects of force/feel system nonlinearities in precipitating undesirable pilot responses such as pilot-induced oscillations (PIOs) has been pointed out by others (e.g., [7]). Note that nonlinearities at the inceptor (pedals) will influence all vehicle responses deriving from pilot-generated rudder inputs. Metric 3 carries the linearity concept to the control loop from applied pedal force to *rudder position*, thus encompassing the dynamics of the force/feel characteristics and rudder actuator at a frequency that may be in evidence in lateral-directional control. Finally, metric 4 addresses the issue of control sensitivity in terms of accelerations, a measure that has long been used in PIO studies (e.g., [8]).

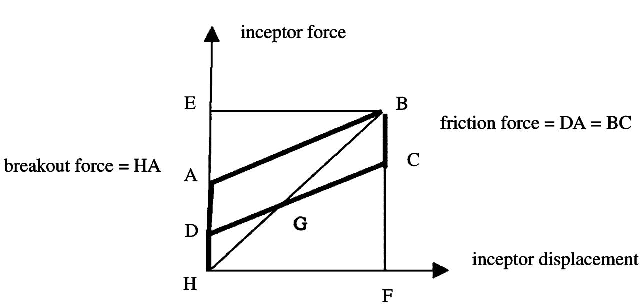

Fig. 2 A linearity index from [3].

Details of the experimental protocol can be found in [2] and will only be described briefly here. The analysis to be presented was not the main thrust of the simulation study summarized in [2]. Here, the metrics of the previous section will be used to delineate safe from possibly unsafe designs, in which safe and unsafe categories will be assigned on the basis of the average pilot-opinion ratings that each configuration received. It should be noted that although metric 4 is intended to be applied at a flight condition of maximum dynamic pressure, it was applied here to the flight condition of the piloted simulation (i.e., landing approach). As was pointed out in the Introduction, the landing approach flight condition involves relatively low dynamic pressure. Of course, if this metric is violated at low dynamic pressure, it most certainly would be at higher dynamic pressures, given the same pedal characteristics.

III. Force/Feel Configurations and Metric Calculation

The 15 different force/feel configurations used in the piloted simulation study are summarized in Table 1. The friction force was kept constant at 1 lbf for all configurations. The damping was 1 lbf/in./s. Values for metrics 2 through 4 were obtained using a simple Simulink® computer model of the force/feel system, actuator, and a baseline measure of lateral acceleration per pound of pedal force beyond breakout. Figure 3 shows the Simulink model. Figure 4 shows a typical, quasi-static pedal-force/displacement plot for configuration 1. Figure 5 shows the dynamic pedal-force/rudder-displacement plot for this configuration. The Appendix includes plots for each of the preceding configurations. The aircraft Dutch-roll natural frequency, necessary for calculating metric 3, was obtained directly from the simulation, by applying a pulsive rudder pedal input and then calculating the natural frequency of the roll-rate response after the rudder inputs were removed. The yaw damper was inoperative in this test. A Dutch-roll frequency of 0.905 rad/s was obtained.

The lateral acceleration at the cockpit per pound of pedal force beyond breakout was determined for one configuration by generating an approximately sinusoidal pedal-force input at 0.9 rad/s and plotting the lateral cockpit acceleration that resulted. The ratio of the maximum applied force (beyond the breakout force) to the maximum lateral acceleration at a number of points was averaged. This yielded

Table 1 Force/feel system characteristics simulated

Configuration	Breakout force, lbf	Force maximum, lbf	Maximum displacement, in.
1	26.5	90	1
2	9.7	47.1	1.43
3	43.3	47.1	1.43
4	9.7	132.9	1.43
5	43.3	132.9	1.43
6	26.5	30	2.5
7	3.0	90	2.5
8–11[a]	26.5	90	2.5
12	50	90	2.5
13	26.5	150	2.5
14	9.7	47.1	3.57
15	43.3	47.1	3.57
16	9.7	132.9	3.57
17	43.3	132.9	3.57
18	26.5	90	4

[a]Configurations 8–11 were identical and were included in the experimental protocol for the purposes of assessing repeatability in ratings.

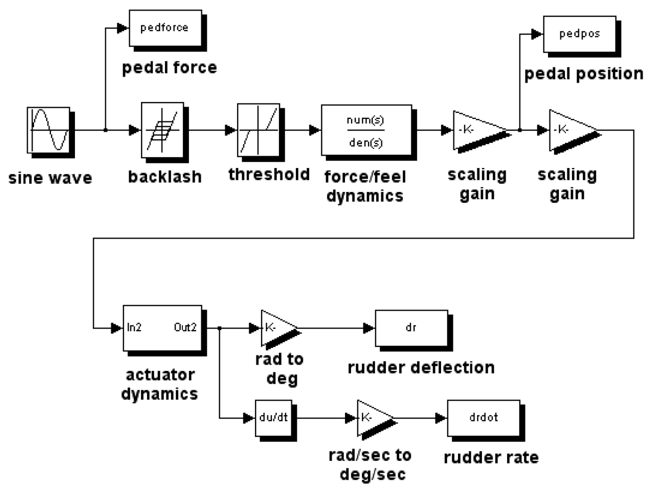

Fig. 3 Simulink model for metric generation.

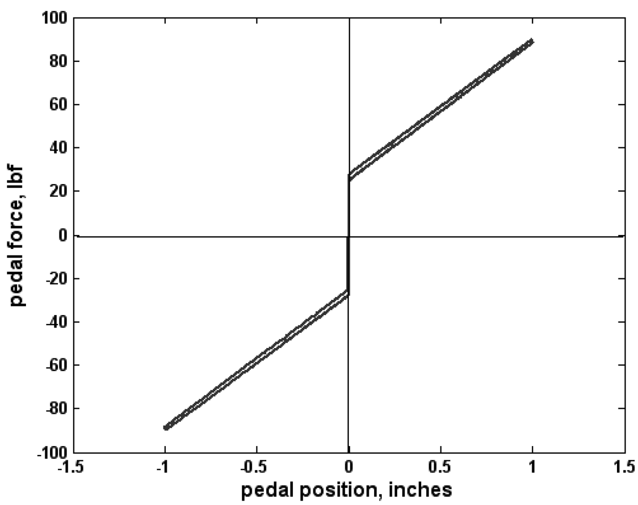

Fig. 4 Quasi-static pedal-force/displacement plot for configuration 1.

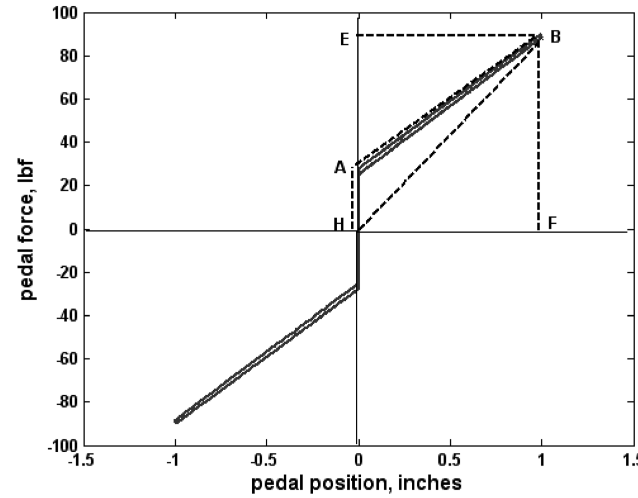

Fig. 6 Calculating the linearity index for a quasi-static deflection.

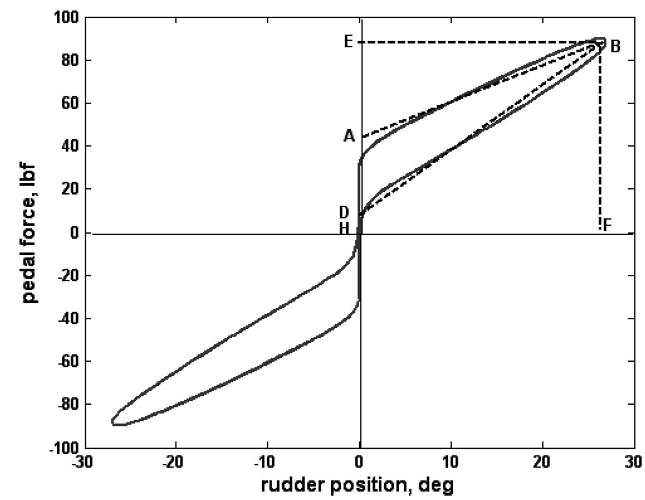

Fig. 7 Calculating the linearity index for a dynamic deflection.

a value of 0.0031 g/lb of pedal force beyond breakout. This value could then be used to determine the acceleration per pound of pedal force beyond breakout for all remaining configurations, knowing the pedal force/feel characteristics of each.

Figure 6 and Eq. (2) indicate how the linearity index of Eq. (1) was obtained for quasi-static deflection cases. Note that the friction force was ignored due to its small size. Figure 7 and Eq. (3) indicate how the linearity index of Eq. (1) was obtained for the dynamic deflection cases.

$$\mathrm{LI} = 1 - \frac{\mathrm{area(HABH)} + \mathrm{area(GBCG)}}{\mathrm{area(HEBF)}} \tag{2}$$

$$\mathrm{LI} = 1 - \frac{\mathrm{area(DABD)}}{\mathrm{area(HEBF)}} \tag{3}$$

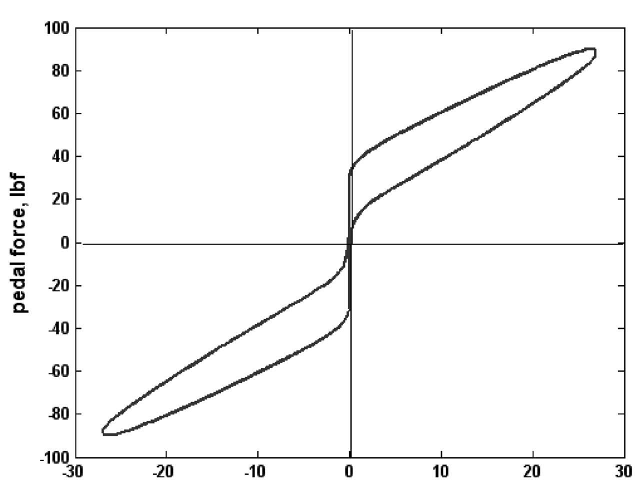

Fig. 5 Dynamic pedal-force/rudder-displacement plot for configuration 1.

The deviation of Fig. 7 and Eq. (3) from Fig. 2 and Eq. (1) is attributable to the curvilinear nature of the plots of pedal force vs rudder position and a desire to simplify the calculation. Obviously, a more accurate calculation could be undertaken.

IV. Metric Evaluation

Average Cooper–Harper (CH) pilot ratings for all pilots for each configuration were obtained as part of the piloted simulation effort. The following normalized rating for each configuration was calculated:

$$\text{normalized rating} = \frac{\text{average CH rating for a configuration}|_{\text{all pilots}}}{\text{largest of the average CH ratings}|_{\text{all pilots, all configurations}}} \tag{4}$$

Table 2 Rating vs metric results

Configuration	Normalized rating	Flagged by a metric?
1	0.83	No[a]
2	0.56	No
3	0.75	Yes
4	0.95	Yes
5	1.0	Yes
6	0.75	Yes
7	0.52	No
8	0.55	No
9	0.55	No
10	0.44	No
11	0.48	No
12	0.96	Yes
13	0.90	Yes
14	0.67	No[a]
15	0.63	Yes
16	0.40	Yes[a]
17	0.71	Yes
18	0.47	No

[a]The metrics failed in an assessment.

Table 3 Rating vs modified metric results

Configuration	Normalized Rating	Flagged by a Metric?
1	0.83	Yes
2	0.56	No
3	0.75	Yes
4	0.95	Yes
5	1.0	Yes
6	0.75	Yes
7	0.52	No
8	0.55	No
9	0.55	No
10	0.44	No
11	0.48	No
12	0.96	Yes
13	0.90	Yes
14	0.67	No[a]
15	0.63	Yes
16	0.40	Yes[a]
17	0.71	Yes
18	0.47	No

[a]The metrics failed in an assessment.

The numerator of Eq. (4) is the average of the Cooper–Harper ratings given by all the pilots to a specific force/feel configuration. The denominator is the grand average of all the Cooper–Harper ratings given by all the pilots for all the configurations. The author is well aware of the pitfalls that are associated with averaging pilot ratings [9]. However, the goal of Eq. (4) was not to delineate handling qualities per se, but rather to provide a single number that described the average relative ranking of the pedal force/feel configurations. Poor or unacceptable force/feel configurations were then interpreted as those having a normalized rating greater than 0.6. Values larger than 0.6 were representative of average Cooper–Harper ratings beyond level 1 (bearing in mind the caveat about averaging ratings just stated).

Table 2 is a comparison of the normalized rating results with the metrics. A *Yes* indicates that the metrics flagged a configuration; a *No* means that the metrics exonerated a configuration. Note that a *Yes* only requires a single metric to be violated. A *No* means that a metric exonerated a configuration (i.e., all metrics were met). Note that although configurations 8–11 were identical, they obtained slightly different normalized ratings. This is not unexpected, because all configurations were presented to the pilots without identification. In addition, the nature of the wind shear may have been different for different runs with the same force/feel configuration.

As the last column of Table 2 indicates, there were three instances in which the metrics gave incorrect results. Two cases occurred in which a configuration with a normalized rating greater than 0.6 were passed, and one case in which a configuration with a normalized rating less than 0.6 was flagged. The most serious error was for configuration 1 in the first row of Table 2. In an attempt to accommodate these cases, an additional metric was created. This was stated as metric 5: a maximum value of lateral acceleration at the cockpit per inch of pedal deflection at the condition of maximum dynamic pressure.

Based upon the data generated in the experiment, a value of 0.25 g/in. of pedal is recommended. Interpreted in the light of metric 4, this added metric could be restated as $(0.005\ g/\mathrm{lbf})/(0.25\ g/\mathrm{in.}$ of pedal), or metric 5: a minimum value of inches of pedal deflection per pound of applied pedal force beyond breakout of 0.02 in./lbf.

Table 3 shows how this added metric effects the results. The more serious error in the first row is now eliminated. Table 4 shows the pass (✓) or fail (X) results for each of the five metrics for each of the configurations. A pass means the configuration met the metric. For example, a pass on metric 1 meant that the maximum pedal force required was less than 100 lbf.

The remaining failure of the metrics is not a minor one: namely, the configuration with the lowest normalized pilot rating (configuration 16) was flagged. This configuration failed one metric: namely, that identifying a maximum required pedal force (132.9 lbf for configuration 16 when compared with the criterion value of 100 lbf). If one were to attempt to correct this "deficiency" by reducing the maximum required pedal force to 100 lbf, a reexamination of the remaining metrics indicates that they would all be met. The question to be asked is whether this 33% reduction in maximum required force would result in a 33% increase in the numerical pilot rating (from 0.40 to 0.6). This question remains open.

Table 4 Metric pass/fail results

Configuration	Metric 1	Metric 2	Metric 3	Metric 4	Metric 5
1	✓	✓	✓	✓	X
2	✓	✓	✓	✓	✓
3	✓	X	X	X	✓
4	X	✓	✓	✓	X
5	X	✓	✓	✓	X
6	✓	X	X	X	✓
7	✓	✓	✓	✓	✓
8–11	✓	✓	✓	✓	✓
12	✓	X	✓	✓	✓
13	✓	X	✓	✓	✓
14	✓	✓	✓	✓	✓
15	✓	X	X	X	✓
16	X	✓	✓	✓	✓
17	X	✓	✓	✓	✓
18	✓	✓	✓	✓	✓

V. Pilot-Induced Oscillations

A. Comparing Two Configurations

Figure 8 shows a time history for configuration 3 for one of the evaluation pilots. As Tables 2 and 3 indicate, this configuration received a normalized rating of 0.75, one of the larger values in the tables. As Table 4 indicates, this configuration also received the maximum number of metric fails for any of the systems (three). As Fig. 8 indicates, a PIO is clearly evident in the time histories. When analyzing the piloted simulation results, a number of such incidents were identified on the basis of cross-spectral measurements between pilot pedal input and aircraft response [2]. Figure 8 indicates 15 s of sustained yaw-rate and pedal-force oscillations with a frequency of 2.5 rad/s. This is one epoch in a series of such oscillations in this run. The corresponding rudder deflections are shown in Fig. 9, in which rudder amplitude-limiting is evident. The predominately right rudder inputs are attributable to the direction of the horizontal wind shear in

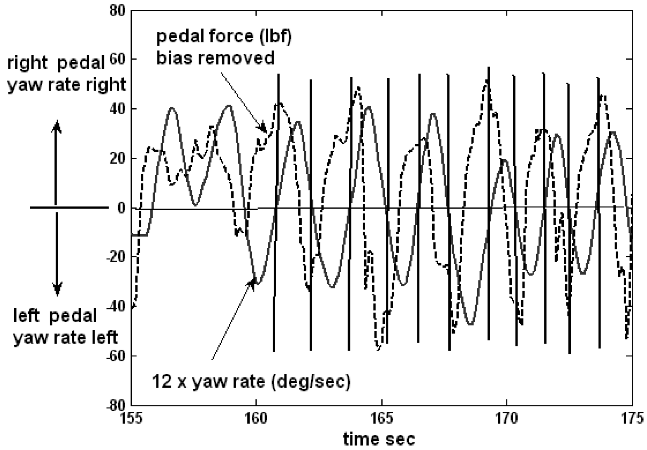

Fig. 8 Yaw-rate and pedal-force time histories for configuration 3 showing a pilot-induced oscillation.

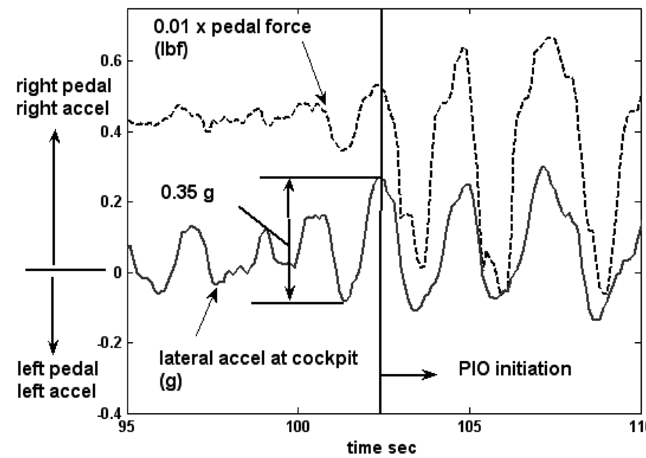

Fig. 10 Initiation of pilot-induced oscillation with configuration 3.

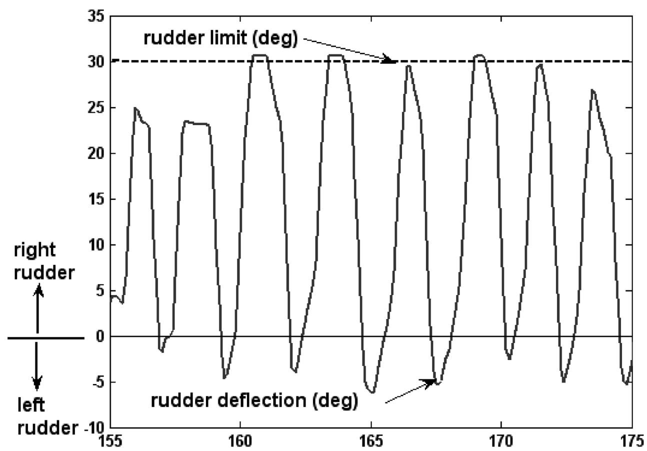

Fig. 9 Rudder deflection time history corresponding to time histories of Fig. 8.

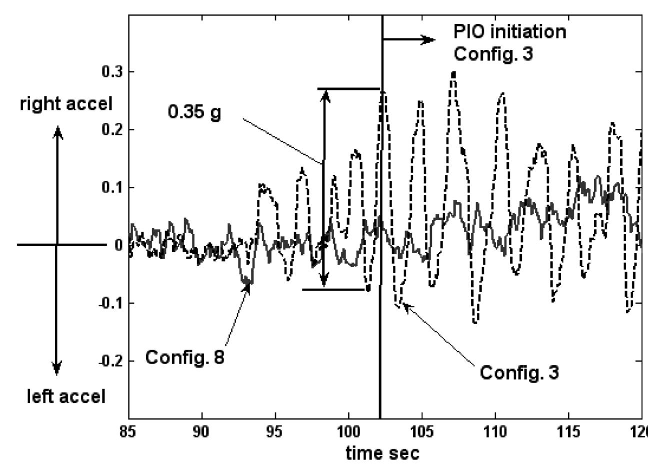

Fig. 11 Comparison of lateral acceleration at the cockpit for same pilot flying configurations 8 and 3.

this simulation run. The vertical lines in Fig. 8 indicate that maximum pedal inputs occur when yaw rate is changing sign. The use of rate control activity in a fully developed PIO was hypothesized to constitute so-called "regressive pilot" behavior in [10]. Indeed, attitude-rate and control-force phasing characteristics such as those of Fig. 8 have been found in other PIO encounters and can be reproduced with the pilot model discussed in [10]. Also of interest is the fact that the PIO frequency is a factor of 2.76 greater than the vehicle's Dutch-roll natural frequency of 0.905 rad/s. A more thorough discussion of PIOs in the simulation is presented in [2].

An interesting question to be asked is, "What might have initiated the PIO?" So-called triggering events have long been associated with the initiation of PIOs [11]. Figure 10 shows time histories of lateral acceleration at the cockpit and pedal-force inputs before and after the PIO was initiated. Note that just before the oscillatory behavior, a large change in lateral acceleration at the cockpit occurred, approximately 0.35 g in magnitude, and this acceleration was attributable to a pedal input. An acceleration of 0.35 g is very large for a transport aircraft and is comparable with that experienced by AA587 before loss of the vertical stabilizer [12]. The author hastens to remind the reader that the piloted simulation was fixed-base in nature. Thus, the pilot's vestibular system did not experience this lateral acceleration.

Figure 11 shows lateral accelerations at the cockpit for the same pilot flying with pedal force/feel configurations 8 and 3. The pedal force/feel characteristics for configuration 8 can also be found in Table 1 and the Appendix. No large pedal-induced lateral accelerations or PIOs occurred in the run with configuration 8. The same wind-shear conditions were in evidence in each of these runs. The probable cause of a large and abrupt pedal input can be surmised by the nature of the pedal force/feel system itself. That is, configuration 3 (see Table 1 and the Appendix) exhibited a large

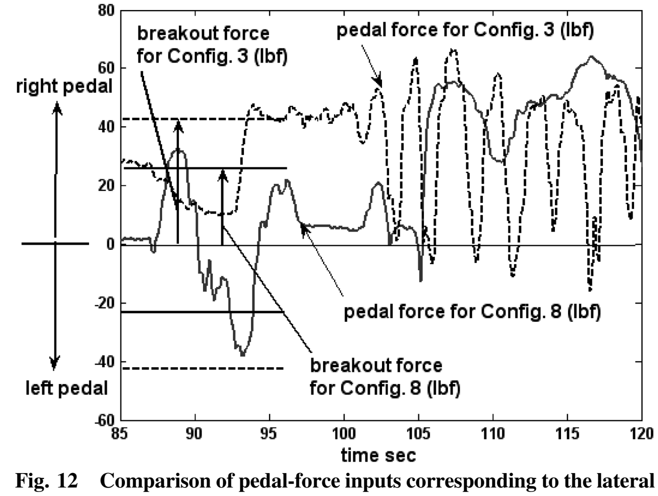

Fig. 12 Comparison of pedal-force inputs corresponding to the lateral accelerations of Fig. 11.

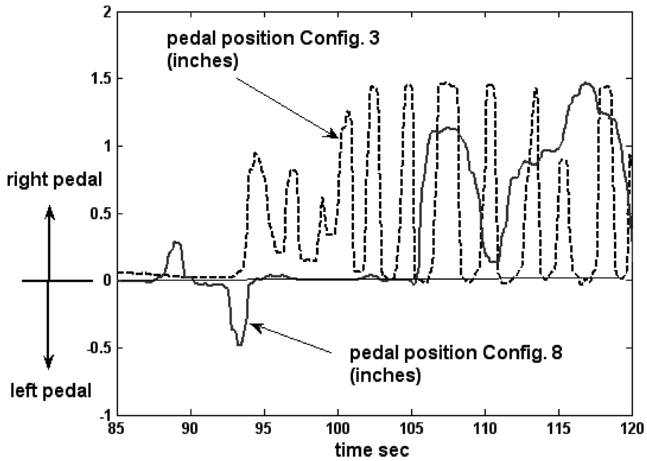

Fig. 13 Comparison of pedal position inputs corresponding to the lateral accelerations of Fig. 11.

pedal breakout force, a small maximum displacement, and a maximum pedal force only 9% larger than the breakout force. The effects of these characteristics are better appreciated by referring to Figs. 12 and 13, in which pedal-force inputs (Fig. 12) and the resulting pedal-position inputs (Fig. 13) corresponding to Fig. 11 are compared. Note in Fig. 12 that both time histories exhibit significant pedal-force inputs. The small force increments above the breakout force for configuration 3 (for 93 s $< t <$ 100 s) yield disproportionately large pedal motions. However, this is not true for configuration 8. This comparison emphasizes the importance of the linearity index in metrics 2 and 3 in Sec. II. Comparing the numerical values for the LIs for metric 2 in each of these cases yields LI $= 0.54$ for configuration 3 and LI $= 0.91$ for configuration 8. Similarlyb comparing metric 3 values for these cases yields LI $= 0.5$ for configuration 3 and LI $= 0.75$ for configuration 8.

B. Discussion

Section V.A focused upon two configurations, one of which obviously exhibited poor force/feel characteristics. It is not surprising that adverse pilot/vehicle interactions occurred with this system, even in a fixed-base simulation. The purpose of focusing upon this particular force/feel system was to emphasize the deleterious effects of poor designs and to demonstrate that the metrics proposed herein are clearly sensitive to these and other deficiencies, as reflected in degraded pilot-opinion ratings. In this manner, it is hoped that the research reported herein can begin to address the NTSB recommendation quoted in the Introduction: that is, to develop "…a certification standard that will ensure safe handling qualities in the yaw axis throughout the flight envelope, including limits for rudder pedal sensitivity."

VI. Conclusions

Based upon the research described herein, the following conclusions can be drawn:

1) A pilot-in-the-loop evaluation of four metrics previously introduced in the literature for evaluation of the safety of transport aircraft force/feel systems suggested that the metrics have merit for identifying force/feel designs that might be prone to pilot-induced oscillations.

2) With the addition of a fifth metric relating maximum cockpit accelerations per inch of pedal deflection, the complete set of five metrics appears to offer promise for application in certification efforts. Taken in consort with the fourth metric, this additional metric can be restated as requiring a minimum value for inches of pedal deflection per pound of pedal force beyond breakout.

3) The metrics must be applied as a set, and each metric must be satisfied for a force/feel configuration to pass the requirements defined by the metrics.

4) When analyzing one of the serious pilot-induced oscillations that occurred in the piloted simulation runs, a hypothesized "triggering event" could be established, consisting of a large lateral acceleration at the cockpit due to a pedal input with a highly nonlinear force/feel system. These undesirable pedal force/feel characteristics were easily identified using the linearity indices discussed herein.

Appendix A: Force/Feel System Characteristics

Figures A1–A15 were used in obtaining the metrics 2 and 3 used in Sec. III.

Configuration 1

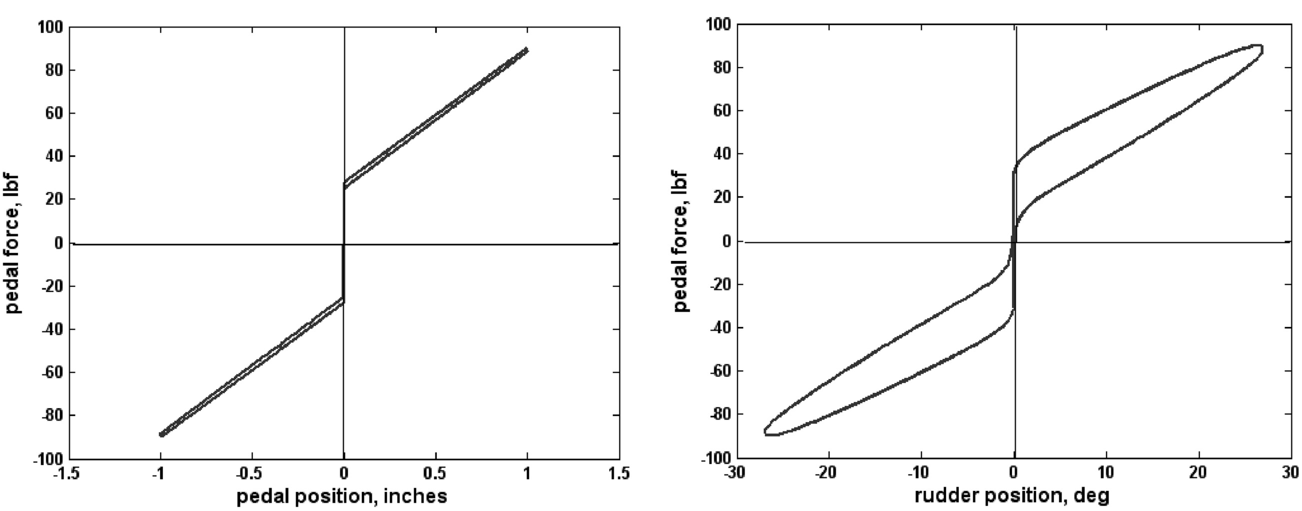

metric (2) metric (3)

Fig. A1 Pedal force vs pedal and rudder positions for configuration 1

Configuration 2

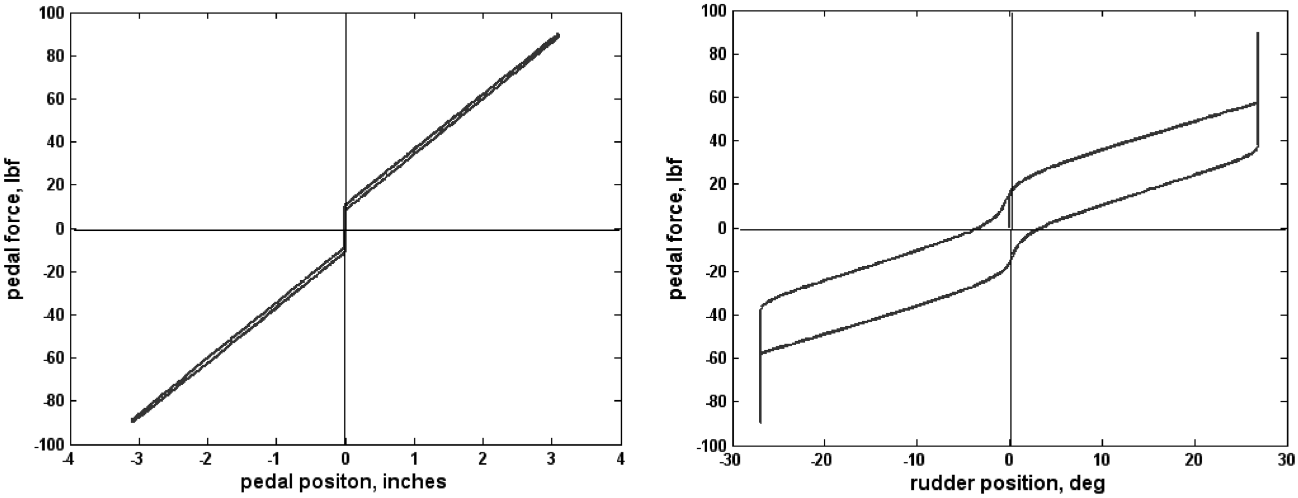

metric (2)

metric (2)

Fig. A2 Pedal force vs pedal and rudder positions for configuration 2

Configuration 3

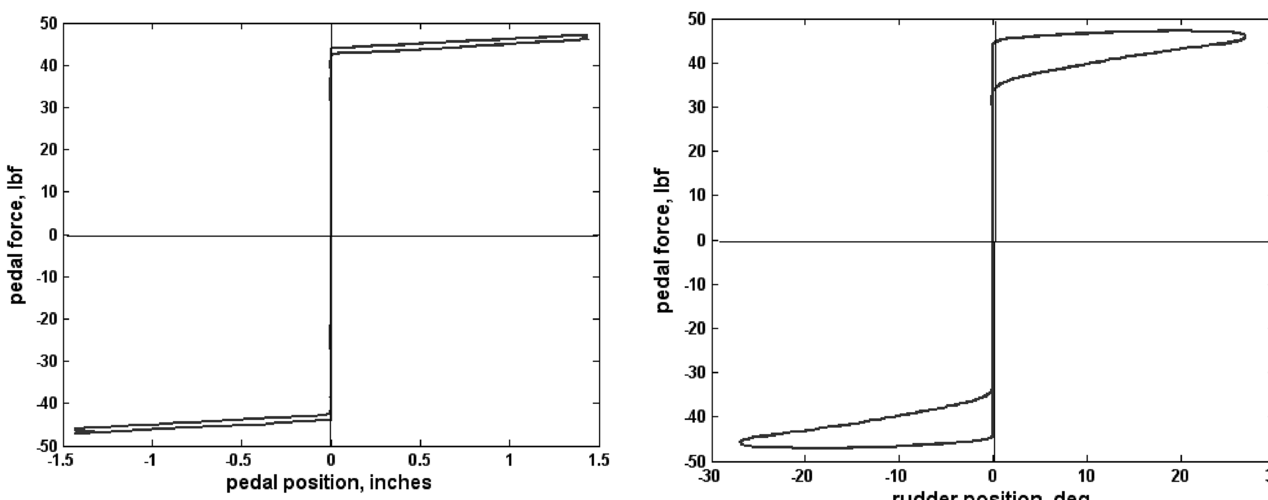

metric (2)

metric (3)

Fig. A3 Pedal force vs pedal and rudder positions for configuration 3.

Configuration 4

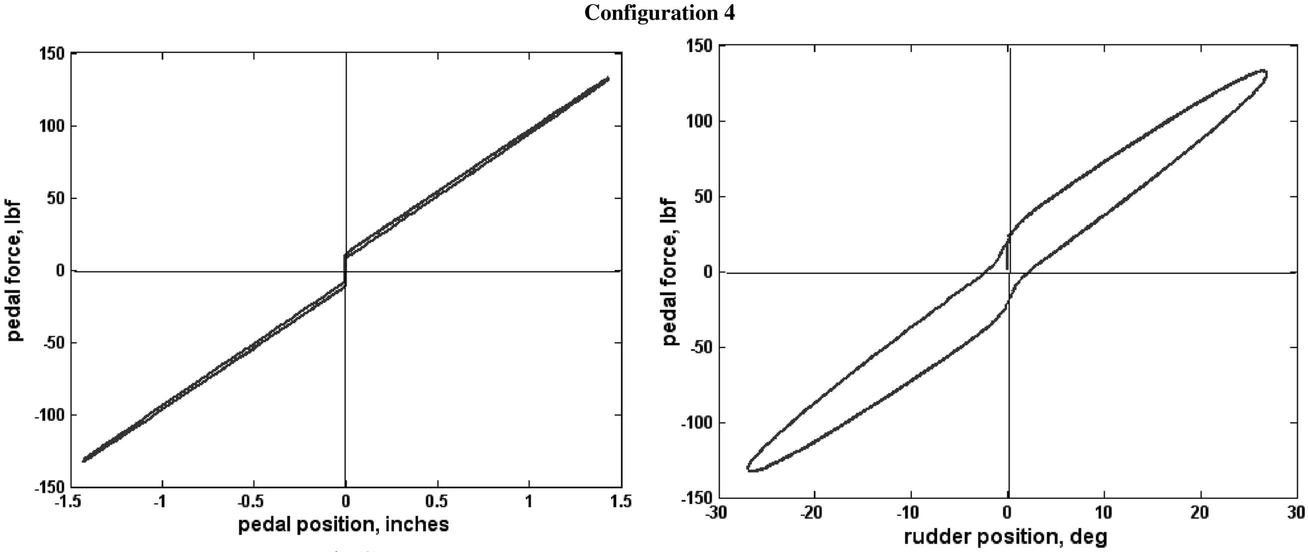

metric (2)

metric (3)

Fig. A4 Pedal force vs pedal and rudder positions for configuration 4.

Configuration 5

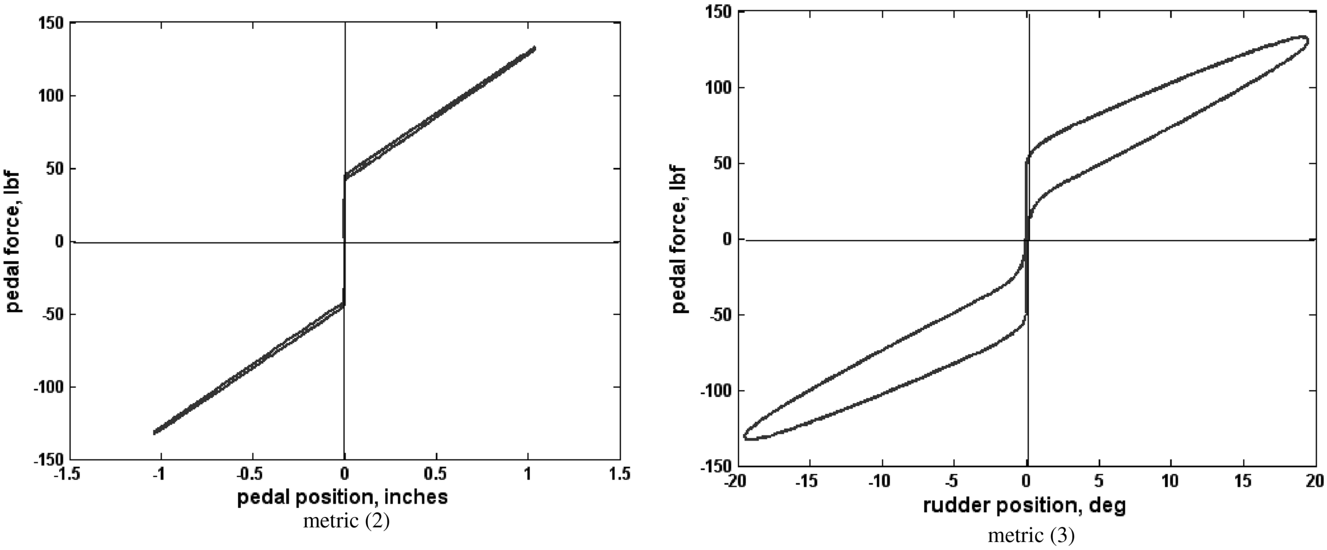

Fig. A5 Pedal force vs pedal and rudder positions for configuration 5.

Configuration 6

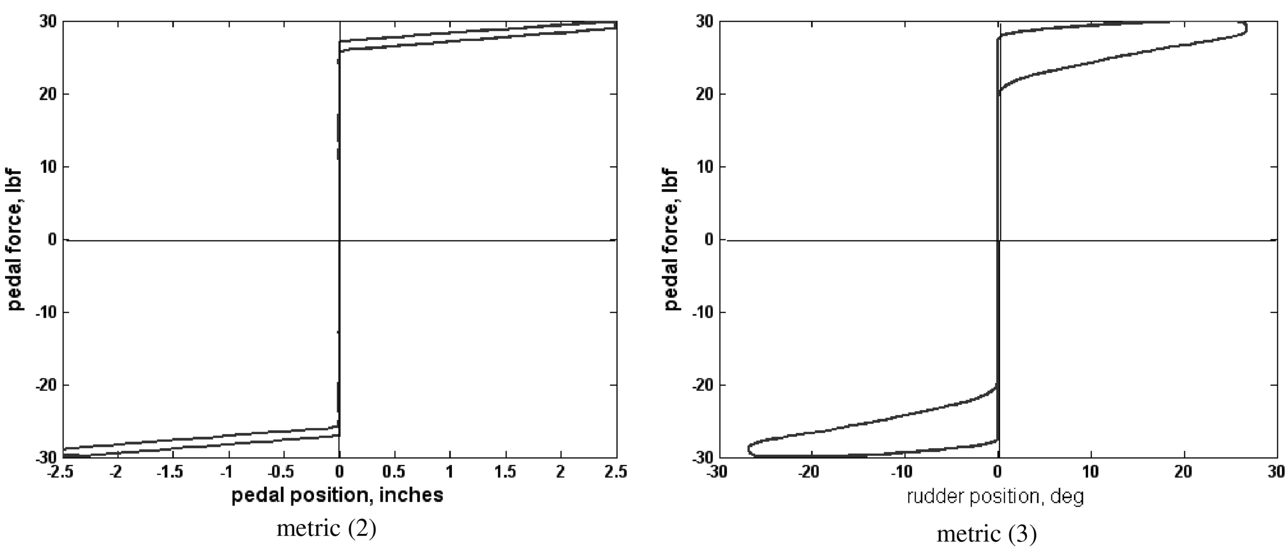

Fig. A6 Pedal force vs pedal and rudder positions for configuration 6.

Configuration 7

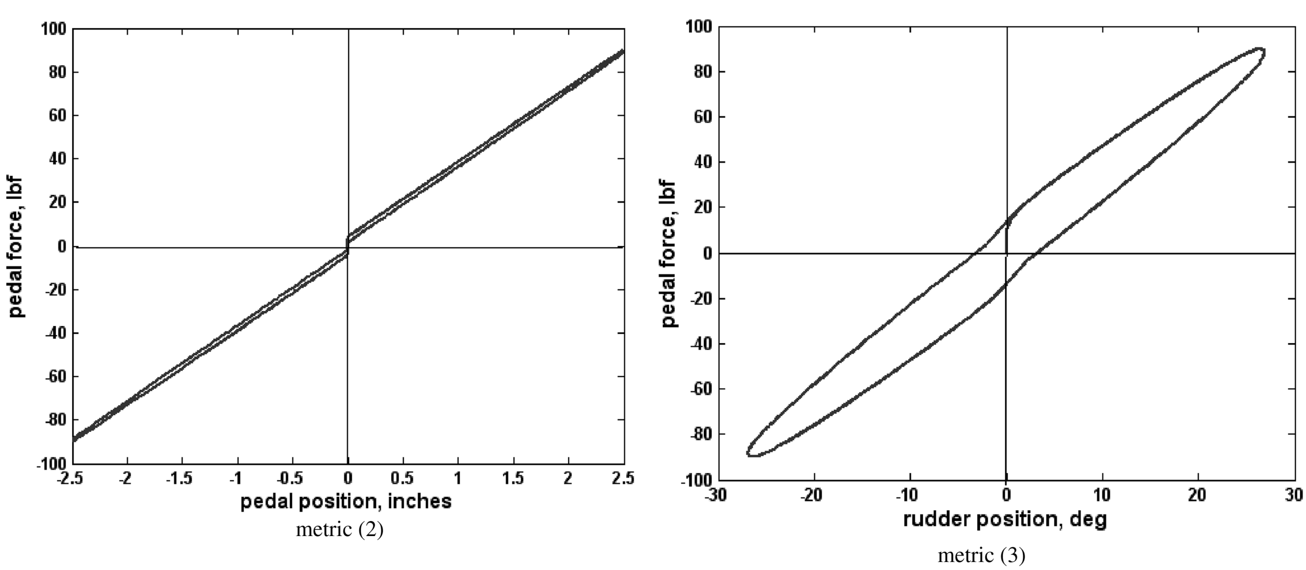

Fig. A7 Pedal force vs pedal and rudder positions for configuration 7.

Configurations 8-11

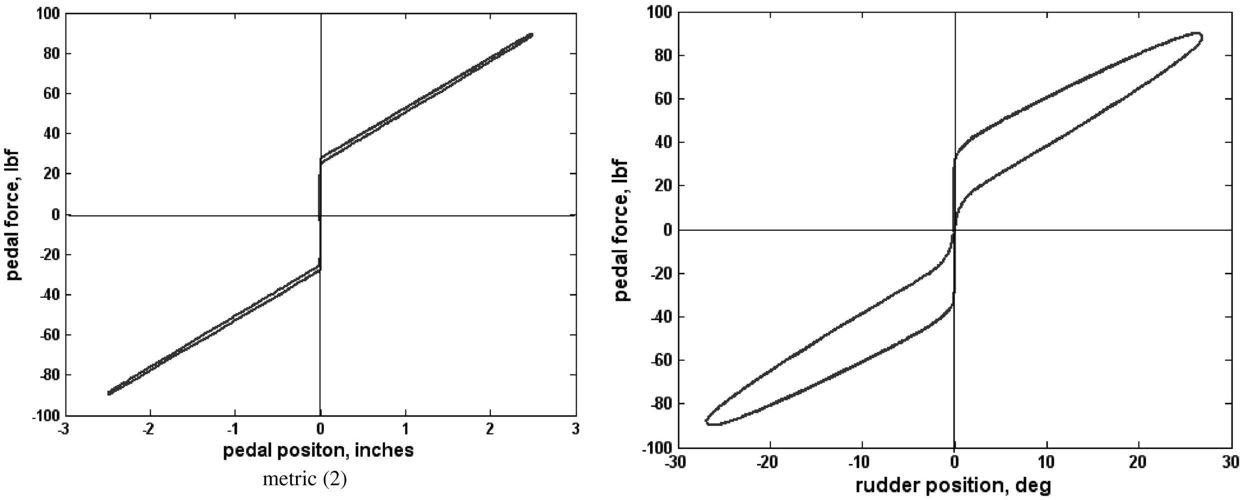

metric (2)

metric (3)

Fig. A8 Pedal force vs pedal and rudder positions for configurations 8–11.

Configuration 12

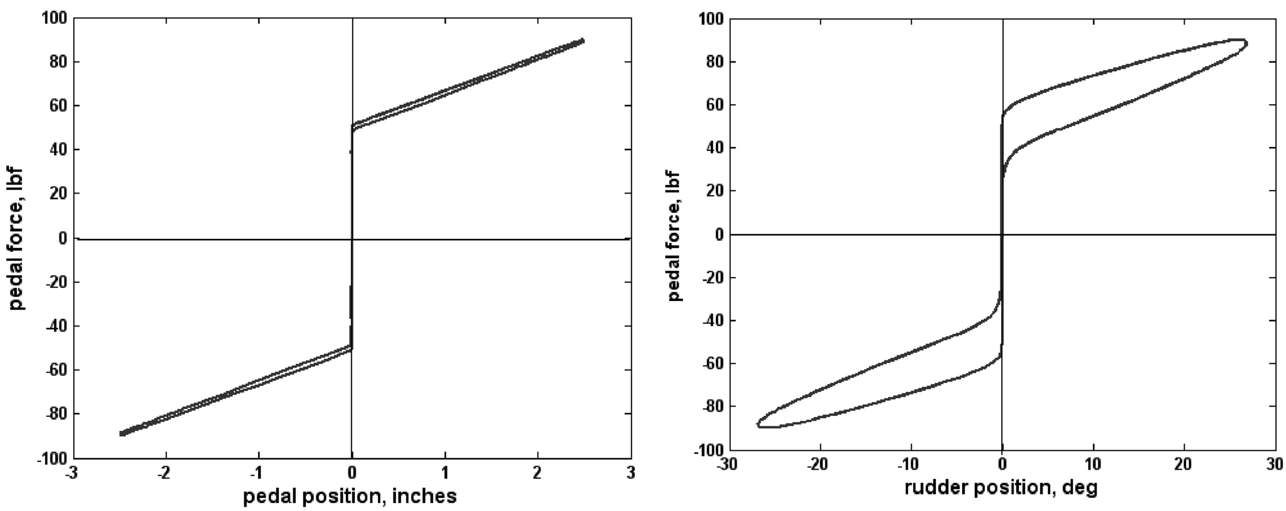

metric (2)

metric (3)

Fig. A9 Pedal force vs pedal and rudder positions for configuration 12.

Configuration 13

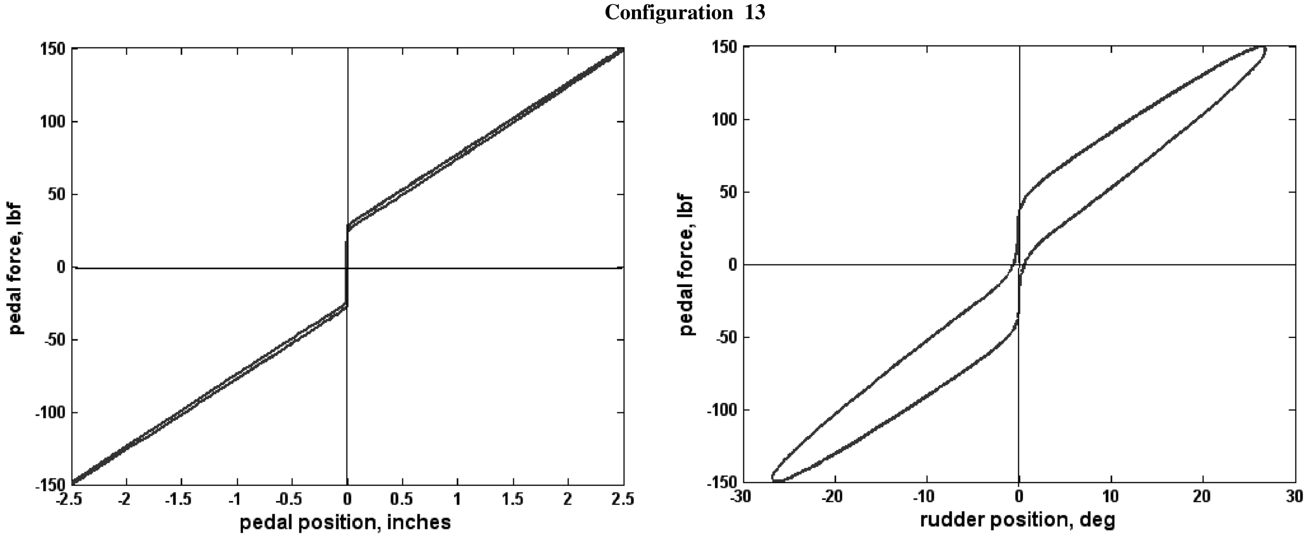

metric (2)

metric (3)

Fig. A10 Pedal force vs pedal and rudder positions for configuration 13.

Configuration 14

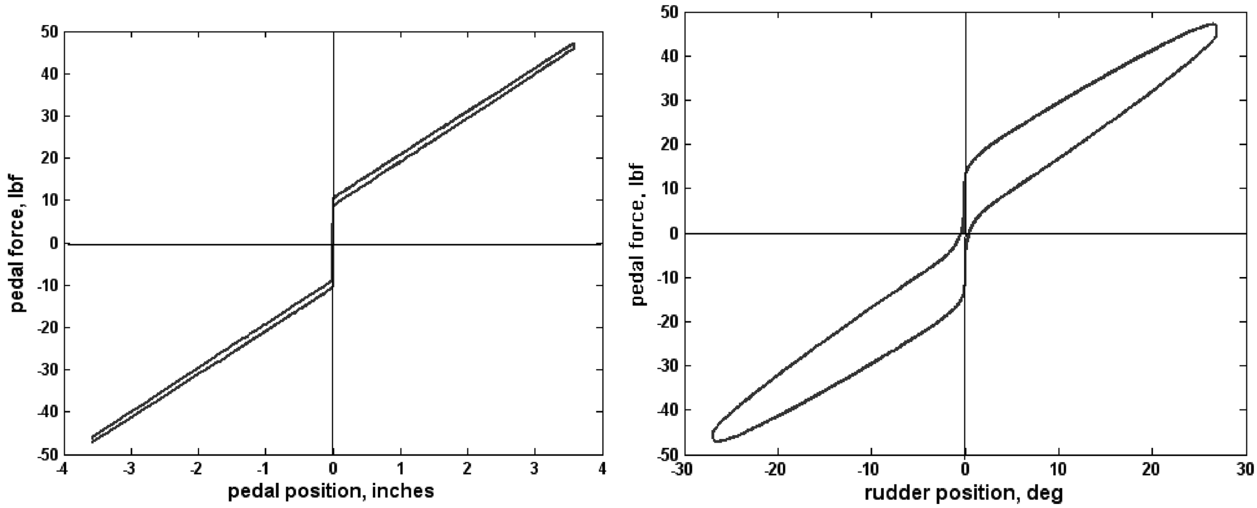

metric (2) metric (3)

Fig. A11 Pedal force vs pedal and rudder positions for configuration 14.

Configuration 15

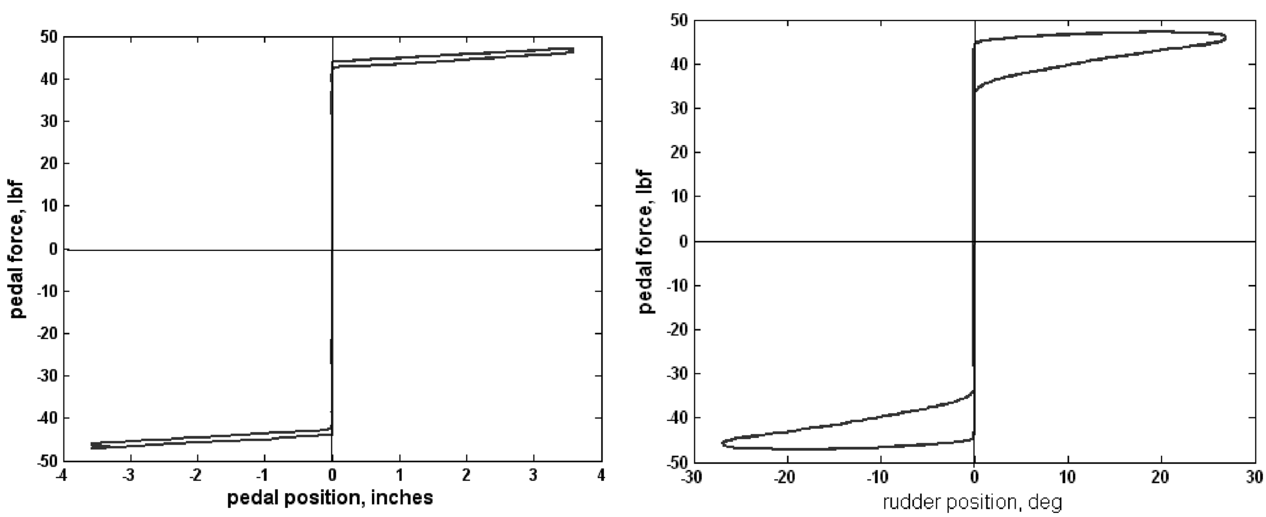

metric (2) metric (3)

Fig. A12 Pedal force vs pedal and rudder positions for configuration 15.

Configuration 16

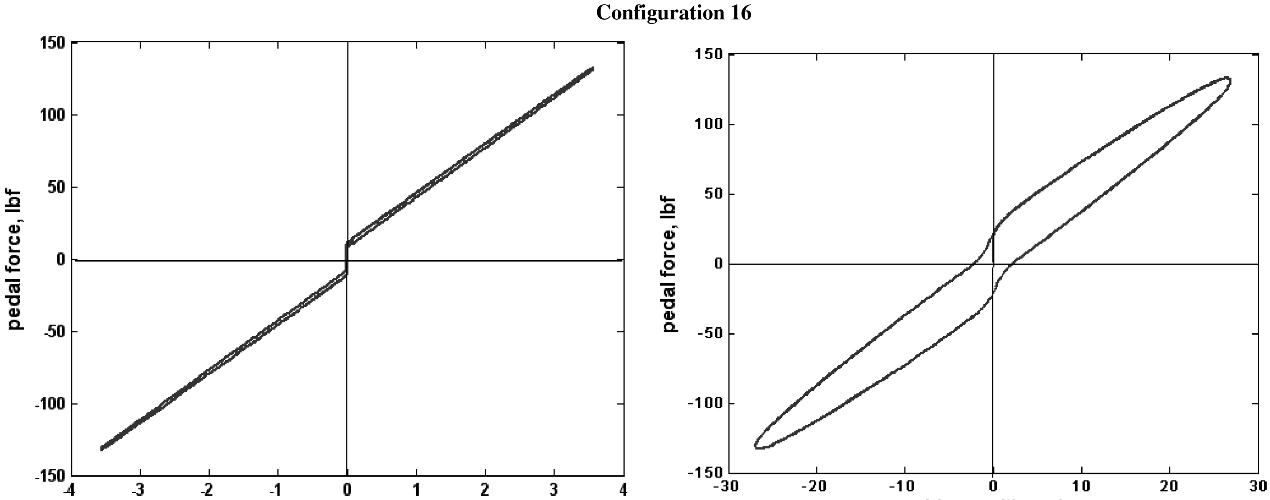

metric (2) metric (3)

Fig. A13 Pedal force vs pedal and rudder positions for configuration 16.

Configuration 17

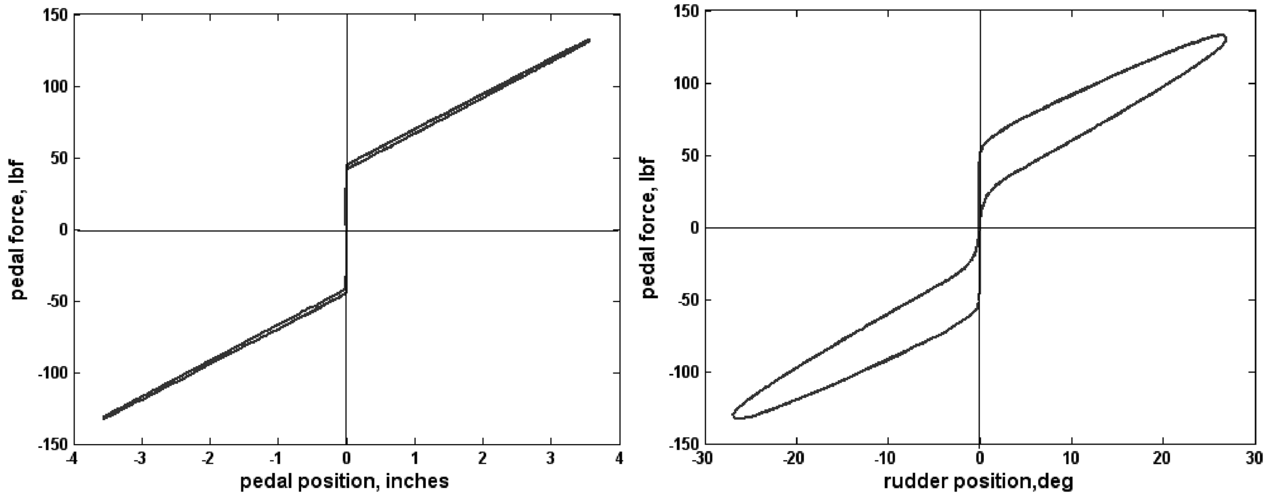

metric (2) metric (2)

Fig. A14 Pedal force vs pedal and rudder positions for configuration 17.

Configuration 18

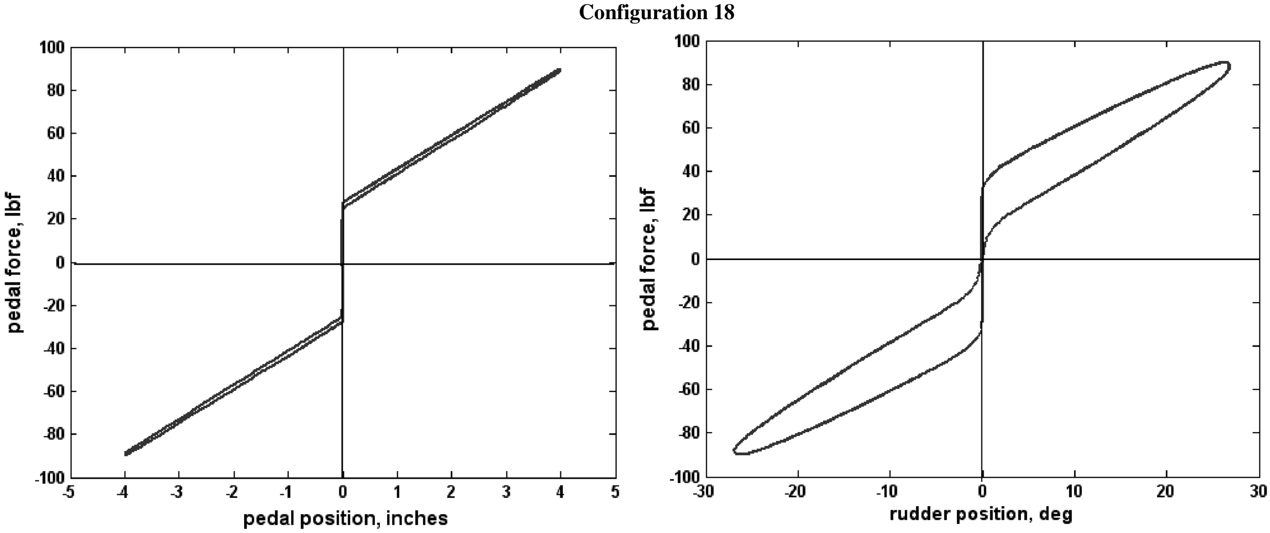

metric (2) metric (3)

Fig. A15 Pedal force vs pedal and rudder positions for configuration 18.

Acknowledgments

This research was supported by NASA Langley Research Center cooperative agreement NNL06-AA04A and by Federal Aviation Administration (FAA) grant DOT FAA 03-6-004. The technical managers for the NASA and FAA grants were Eric Stewart and Robert McGuire, respectively. The conclusions drawn in this study are those of the author and do not necessarily reflect those of NASA or the FAA.

References

[1] Anon., "Aircraft Accident Report: In-Flight Separation of Vertical Stabilizer, American Airlines Flight 587, Airbus Industrie A300-605R, N14053, Belle-Harbor, New York, November 12, 2001," National Transportation Safety Board, Rept. NTSB/AAR-04/04, Washington, DC, 26 Oct. 2004.

[2] Stewart, E. C., "A Piloted Simulator Evaluation of Transport Aircraft Rudder Pedal Force/Feel Systems," *98th SAE Aerospace Control and Guidance Systems Committee Meeting* [CD-ROM], Society of Automotive Engineers, Warrendale, PA, Oct. 2006.

[3] Kaiser, M. K., and Schroeder, J. A., "Flights of Fancy: The Art and Science of Flight Simulation," *Principles and Practice of Aviation Psychology*, edited by P. S. Tsang and M. A. Vidulich, Lawrence Erlbaum Associates, Mahwah, NJ, 2003.

[4] Lee, B., Rodchenki, V., Zaichik, L., and Yashin, Y., "Effect of Pedal Feel System Characteristics on Aircraft HQ," AIAA Atmospheric Flight Mechanics Conference and Exhibit, San Francisco, AIAA Paper 2005-6034, 15–18 Aug. 2005.

[5] Hess, R. A., "Certification and Design Issues for Rudder Control Systems in Transport Aircraft," *Journal of Guidance, Control, and Dynamics*, Vol. 29, No. 5, 2006, pp. 1210–1220. doi:10.2514/1.18715

[6] Hess, R. A., "Rudder Control Strategies and Force-Feel System Designs in Transport Aircraft," *Journal of Guidance, Control, and Dynamics*, Vol. 28, No. 6, 2005, pp. 1251–1262.

[7] Weltz, G. L., Shweyk, K. M., and Murray, D. M., "Application of New and Standard Pilot-Induced Oscillation (PIO) Analysis Methods to Flight Test Data of the C-17 Transport Aircraft," AIAA Atmospheric Flight Mechanics Conference and Exhibit, Hilton Head, SC, AIAA Paper 2007-6387, 20–23 Aug. 2007.

[8] Mitchell, D. G., and Klyde, D. H., "Bandwidth Criteria for Category I and II PIOs," *Pilot-Induced Oscillation Research: Status at the End of the Century*, NASA Rept. CP-2001-210389, Vol. 1, Apr. 2001, pp. 17–19.

[9] Hess, R. A., "Nonadjectival Rating Scales in Human Response Experiments," *Human Factors*, Vol. 15, No. 3, 1973, pp. 275–280.

[10] Hess, R. A., "Unified Theory for Aircraft Handling Qualities and Adverse Aircraft-Pilot Coupling," *Journal of Guidance, Control, and Dynamics*, Vol. 20, No. 6, 1997, pp. 1141–1148.

[11] Anon., *Aviation Safety and Pilot Control, Understanding and Preventing Unfavorable Pilot-Vehicle Interactions*, National Academy Press, Washington, DC, 1997.

[12] Hess, R. A., "An Inquiry into Whether a Pilot-Induced Oscillation Was a Factor in the Crash of American Airlines Flight 587," National Transportation Safety Board, Rept. 288388, Washington, DC, Dec. 2003; also available at http://www.ntsb.gov/events/2001/AA587/exhibits/288388.pdf [retrieved 14 November 2007].